JACS
JOURNAL OF THE AMERICAN CHEMICAL SOCIETY
Article
pubs.acs.org/JACS

Structure and Magnetism of $Sr_3Co_2O_4Cl_2$—An Electronically Driven Lattice Distortion in an Oxychloride Containing Square Planar Co^{II} Centers

Fabio Denis Romero, Lucy Coyle, and Michael A. Hayward*

Department of Chemistry, Inorganic Chemistry Laboratory, University of Oxford, South Parks Road, Oxford, OX1 3QR, United Kingdom

Supporting Information

ABSTRACT: Topochemical reduction of $Sr_3Co_2O_5Cl_2$ with NaH at 200 °C yields $Sr_3Co_2O_4Cl_2$, a phase consisting of infinite double sheets of corner-linked $Co^{II}O_4$ square planes stacked with SrCl rocksalt layers. At 298 K, the structure of $Sr_3Co_2O_4Cl_2$ is described in the tetragonal space group $I4/mmm$ [a = 4.007(1) Å, c = 22.282(1) Å]; however, on cooling below 200 K, the structure undergoes a lattice distortion to adopt a structure with orthorhombic symmetry in space group $Immm$ [a = 3.9757(5) Å, b = 4.0294(5) Å, and c = 22.147(3) Å at 5 K]. The structural distortion can be considered Jahn–Teller-like as it lifts the orbital degeneracy of the square planar, d^7, Co^{II} centers, demonstrating a strong coupling between the electronic configuration and the structural lattice of this oxychloride phase. On cooling below 50 K, $Sr_3Co_2O_4Cl_2$ adopts a canted antiferromagnetically ordered state. All magnetization data show that the local cobalt moment is much greater than would be expected for a simple spin-only $S = {}^3/_2$ center, indicating a strong orbital contribution to the magnetic behavior.

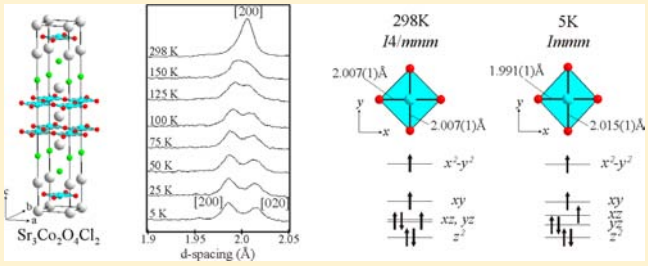

INTRODUCTION

Extended solids containing highly connected transition metal-anion lattices are of great interest due to the wide variety of complex electronic and magnetic behavior they exhibit. This complex behavior is principally due to the presence of electrons in partially filled d-states, which interact strongly with each other through the metal-anion framework to form correlated electronic states that can give rise to exotic behavior such as superconductivity or magnetoresistance. The electronic structure of such a system is a function of the transition metal valence electron count and local coordination, which define the local transition metal electronic configuration, and the long-range metal-anion lattice structure, which defines the nature and strength of the electronic coupling between metal centers. Thus, by modifying and controlling these features of extended solids, we can tune the electronic structure of materials and thus their physical behavior.

Low-temperature topochemical reduction reactions performed on transition metal oxides and oxyhalides, using binary metal hydrides as reducing agents, have enabled the preparation of novel extended solid phases that contain transition metal cations in unusual oxidation states and coordination geometries, such as square planar Ni^I and Co^I or octahedral Mn^I.[1-3]

Using this strategy we have recently shown that the topochemical reduction of the oxychloride phase $Sr_3Fe_2O_5Cl_2$ yields the Fe(II) phase $Sr_3Fe_2O_4Cl_2$, which consists of infinite sheets of corner-linked $Fe^{II}O_4$ square planes stacked with SrCl rocksalt layers, as shown in Figure 1.[4] The $Sr_3B_2O_5Cl_2$ framework appears to selectively direct the reduction reaction to remove the central bridging oxide ion to form products containing sheets of $B^{II}O_4$ centers, in a manner that appears indifferent to the transition metal B-cation valence electron count. Thus, a series of isostructural $Sr_3Fe_{2-x}Co_xO_4Cl_2$ ($0 \le x \le$

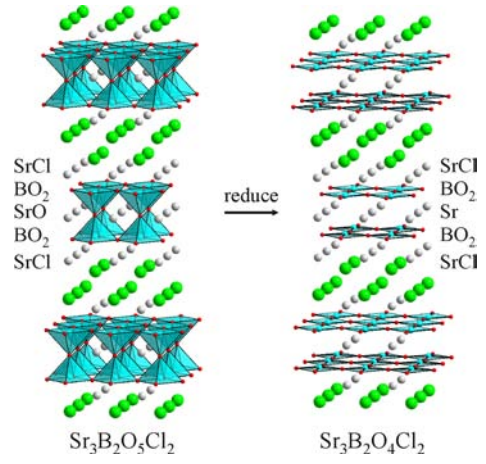

Figure 1. Topochemical reduction of $Sr_3B_2O_5Cl_2$ (B = Fe, Co) leads to the deintercalation of the central bridging oxide ion and the formation of $Sr_3B_2O_4Cl_2$ consisting of infinite sheets of $B^{II}O_4$ square planes stacked with SrCl rocksalt layers.

Received: July 9, 2012
Published: August 29, 2012

   dx.doi.org/10.1021/ja306683y | J. Am. Chem. Soc. 2012, 134, 15946–15952

1) phases can be prepared by the reduction of the analogous $Sr_3Fe_{2-x}CoO_4Cl_2$ phases.[5] The importance of the structure-directing role of the $Sr_3B_2O_5Cl_2$ lattice in controlling the selectivity of reduction reactions can be seen by making a comparison to the reaction used to prepare the infinite layer phase $SrFeO_2$ by the reduction of $SrFeO_3$.[6] In this instance, only 30% cobalt substitution leads to a change in the structure of the reduced product phase, suggesting the selectivity of the reduction reaction is strongly dependent on the metal valence electron count in this case.[7] Here we report the synthesis, structure, and physical behavior of the $x = 2$ end member of the $Sr_3Fe_{2-x}Co_xO_4Cl_2$ series, $Sr_3Co_2O_4Cl_2$.

EXPERIMENTAL SECTION

Preparation of $Sr_3Co_2O_5Cl_2$. Samples of $Sr_3Co_2O_5Cl_2$ were prepared by the route previously described by Weller et al. for the synthesis of $Sr_3FeCoO_5Cl_2$.[8] Suitable stoichiometric quantities of SrO (prepared by decomposition of $SrCO_3$ at 1100 °C under vacuum), $SrCl_2$ (dried at 180 °C under vacuum), and $Sr_2Co_2O_5$ (prepared using the method described by Grenier et al.[9]) were thoroughly mixed using an agate mortar and pestle in an argon-filled glovebox (O_2 and H_2O < 1 ppm). The resulting mixtures were then sealed under vacuum in silica ampules and heated at 850 °C for two periods of 24 h with one intermediate grinding. X-ray powder diffraction data collected from the resulting samples were consistent with single-phase materials with lattice parameters [a = 3.91(1) Å and c = 24.00(1) Å] in good agreement with literature values.[10]

Reduction of $Sr_3Co_2O_5Cl_2$. The reduction of $Sr_3Co_2O_5Cl_2$ was performed using NaH as a solid-state reducing agent.[1] Small samples (approximately 200 mg) of $Sr_3Co_2O_5Cl_2$ were ground together with a double molar excess of NaH in an argon-filled glovebox. The mixtures were then sealed under vacuum in Pyrex ampules and heated to temperatures between 170 and 300 °C to monitor the temperature dependence of the reduction reactions. Large samples suitable for neutron diffraction measurements were synthesized in the same manner and heated for two periods of 2 days at 200 °C with an intermediate grinding. After reaction, samples were washed under nitrogen with 2 × 100 mL aliquots of 0.1 M NH_4Cl in methanol, followed by 4 × 100 mL aliquots of methanol to remove unwanted reaction byproducts (NaH and NaOH).

Characterization. Room-temperature X-ray powder diffraction data were collected from samples contained in gas-tight sample holders using a PANalytical X'Pert diffractometer incorporating an X'celerator position sensitive detector (monochromatic Cu Kα1 radiation). Variable-temperature X-ray powder diffraction data were collected using a Siemens D5000 diffractometer using an Oxford Cryosystems PheniX cryostat. Neutron powder diffraction data were collected from samples contained within vanadium cans sealed under argon with indium washers using the POLARIS instrument at the ISIS neutron source (UK) and the D2b diffractometer (λ = 1.59 Å) at the ILL (France). Rietveld profile refinements were performed using the GSAS suite of programs.[11] Magnetization data were collected using a Quantum Design MPMS SQUID magnetometer. Magnetization data indicated that all the reduced samples contained small quantities of ferromagnetic elemental cobalt, which masked the magnetic behavior of the bulk phases. The paramagnetic susceptibility and saturated ferromagnetic moment of samples were therefore measured using a "ferromagnetic subtraction" technique described previously[12] and described fully in the Supporting Information.

RESULTS

Reactivity of $Sr_3Co_2O_5Cl_2$. X-ray powder diffraction data collected from the products of reaction between $Sr_3Co_2O_5Cl_2$ and NaH reveal that reactions performed at temperatures in the range 170 < T/°C < 240 resulted in the formation of body-centered tetragonal phases with lattice parameters similar to those of $Sr_3Fe_2O_4Cl_2$, indicating that the topochemical reduction of $Sr_3Co_2O_5Cl_2$ had occurred. Reaction temperatures greater than 240 °C resulted in the formation of elemental cobalt and a complex mixture of binary oxides and chlorides.

Examination of X-ray powder diffraction data collected from reduction products before and after washing with methanol revealed that a significant quantity of the reduction product (~50% by weight) was being reoxidized back to the $Sr_3Co_2O_5Cl_2$ starting phase during this procedure. The degree of reoxidation during the washing procedure was mitigated by the use of a slightly acidic solvent (0.1 M NH_4Cl in methanol) to prevent oxidation of the product by hydroxide ions generated during the dissolution of NaOH ($2OH^- \rightarrow H_2O + O^{2-}$); however, reoxidation during the washing step could not be completely eliminated. This high degree of air-sensitivity is consistent with the pyrophoric behavior of $Sr_3Fe_{2-x}Co_xO_4Cl_2$ phases observed previously.[4,5]

Structural Characterization of $Sr_3Co_2O_4Cl_2$ at 298 K. X-ray powder diffraction data collected from the washed products of reaction between $Sr_3Co_2O_5Cl_2$ and NaH performed at 200 °C could be readily indexed on the basis of a body-centerd tetragonal unit cell [a = 4.007(1) Å, c = 22.282(1) Å], consistent with the topochemical reduction of $Sr_3Co_2O_5Cl_2$ to $Sr_3Co_2O_4Cl_2$.

Neutron powder diffraction data collected at room temperature (POLARIS) from $Sr_3Co_2O_4Cl_2$ could be readily indexed with a body-centered tetragonal unit cell similar to that of $Sr_3Fe_{2-x}Co_xO_4Cl_2$ ($0 \le x \le 1$) phases.[4,5] A structural model based on the refined structure of $Sr_3Fe_2O_4Cl_2$ was therefore constructed and refined against these data. As noted above, the sample contained a small amount of $Sr_3Co_2O_5Cl_2$ impurity. This was therefore added as a second phase to the structural refinement. The refinement converged readily to give a good statistical fit (χ^2 = 2.506). Attempts to reinsert an oxide ion into the "bridging" site of the structural model were unsuccessful, with the occupancy of this site consistently refining to zero, confirming the composition of the bulk phase as $Sr_3Co_2O_4Cl_2$. Full details of the refined structure of $Sr_3Co_2O_4Cl_2$ are given in Table 1 with selected bond lengths in Table 2. Observed, calculated, and difference plots from the refinement of $Sr_3Co_2O_4Cl_2$ against room temperature neutron powder diffraction data are shown in the Supporting Information.

Table 1. Refined Structural Parameters of $Sr_3Co_2O_4Cl_2$ at 298 K

atom	Wyckoff position	x	y	z	U_{iso} (Å^2)
Sr(1)	2a	0	0	0	0.0033(7)
Sr(2)	4e	0	0	0.1526(1)	0.0038(5)
Co(1)	4e	0	0	0.4284(4)	0.0085(8)
O(1)	8g	1/2	0	0.0766(1)	0.0161(3)
Cl(1)	4e	0	0	0.2960(1)	0.0202(4)

$Sr_3Co_2O_4Cl_2$: space group $I4/mmm$, a = 4.007(1) Å, c = 22.282(8) Å, weight fraction = 89.7%

$Sr_3Co_2O_5Cl_2$: space group $I4/mmm$, a = 3.987(1) Å, c = 22.817(10) Å, weight fraction = 10.3%

χ^2 = 2.506, wRp = 0.64%, Rp = 0.90%

Structural Characterization of $Sr_3Co_2O_4Cl_2$ at 5 K. Neutron powder diffraction data (POLARIS) collected from $Sr_3Co_2O_4Cl_2$ exhibited a splitting of diffraction peaks relative to the data collected at 298 K, consistent with an orthorhombic distortion of the unit cell (Figure 2). The 5 K data set could be readily indexed using a body-centered orthorhombic unit cell [a

dx.doi.org/10.1021/ja306683y | J. Am. Chem. Soc. 2012, 134, 15946−15952

Table 2. Selected Bond Lengths from the Refined Structure of $Sr_3Co_2O_4Cl_2$ at 298 K

cation	anion	bond length (Å)	Bond Valence Sum
Co(1)	O(1)	2.007(1) × 4	Co + 1.79
	Cl(1)	2.950(2)	
Sr(1)	O(1)	2.632(2) × 8	Sr + 1.99
Sr(2)	O(1)	2.623(1) × 4	Sr + 2.09
	Cl(1)	3.056(1) × 4	
	Cl(1)	3.195(3)	
Co	Co	3.19(1)	

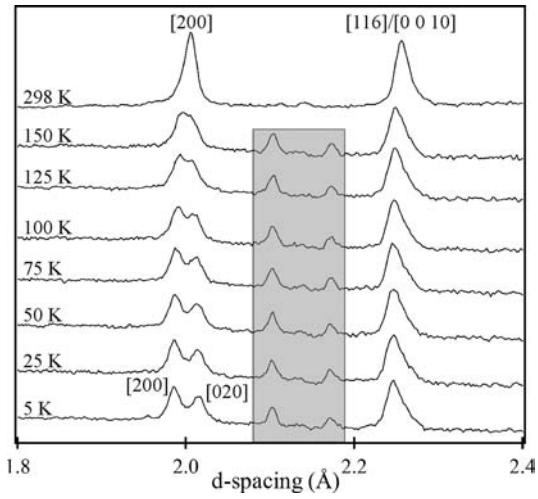

Figure 2. Neutron powder diffraction data (POLARIS) collected from $Sr_3Co_2O_4Cl_2$ as a function of temperature. Splitting of the [200] diffraction peak but not [116] or [0010] indicates a orthorhombic distortion at low temperature. Peaks at 2.10 and 2.17 Å in the shaded box correspond to contributions from the cryostat.

= 3.9757(5) Å, b = 4.0294(5) Å, and c = 22.147(3) Å]; therefore, an orthorhombic model (space group *Immm*) based on the room-temperature structure of $Sr_3Co_2O_4Cl_2$ was constructed and refined against these low-temperature data. The refinement converged rapidly to yield a good statistical fit (χ^2 = 3.23). Full structural details of the 5 K structure of $Sr_3Co_2O_4Cl_2$ are described in Table 3, with selected bond lengths in Table 4. Observed, calculated, and difference plots from the refinement are shown in the Supporting Information.

Additional neutron diffraction data (D2b) collected from $Sr_3Co_2O_4Cl_2$ at 5 K, with increased sensitivity to large d-spacing features, were observed to exhibit additional diffraction features

Table 3. Refined Structural Parameters of $Sr_3Co_2O_4Cl_2$ at 5 K

atom	Wyckoff position	x	y	z	U_{iso} (Å^2)
Sr(1)	2a	0	0	0	0.0014(3)
Sr(2)	4i	0	0	0.1528(1)	0.0014(3)
Co(1)	4i	0	0	0.4276(3)	0.0090(5)
O(1)	4j	1/2	0	0.0749(4)	0.0094(5)
O(2)	4j	0	1/2	0.0773(4)	0.0094(5)
Cl(1)	4i	0	0	0.2952(1)	0.0110(5)

$Sr_3Co_2O_4Cl_2$: space group *Immm*, a = 3.9757(5) Å, b = 4.0294(5) Å, c = 22.147(3) Å, weight fraction = 89.7%

$Sr_3Co_2O_3Cl_2$: space group *I*4/*mmm*, a = 3.983(1) Å, c = 22.720(10) Å, weight fraction = 10.3%

χ^2 = 3.230; wRp = 0.55%; Rp = 0.67%

Table 4. Selected Bond Lengths from the Refined Structure of $Sr_3Co_2O_4Cl_2$ at 5 K

cation	anion	bond length (Å)	Bond Valence Sum
Co(1)	O(1)	2.015(1) × 2	Co + 1.82
	O(2)	1.991(1) × 2	
	Cl(1)	2.932(7)	
Sr(1)	O(1)	2.589(6) × 4	Sr + 2.08
	O(2)	2.644(6) × 4	
Sr(2)	O(1)	2.632(6) × 2	Sr + 2.10
	O(2)	2.618(6) × 2	
	Cl(1)	3.056(1) × 4	
	Cl(1)	3.154(3)	
Co	Co	3.20(1)	

relative to analogous data collected at 298 K, consistent with the presence of long-range magnetic order (Figure 3). These

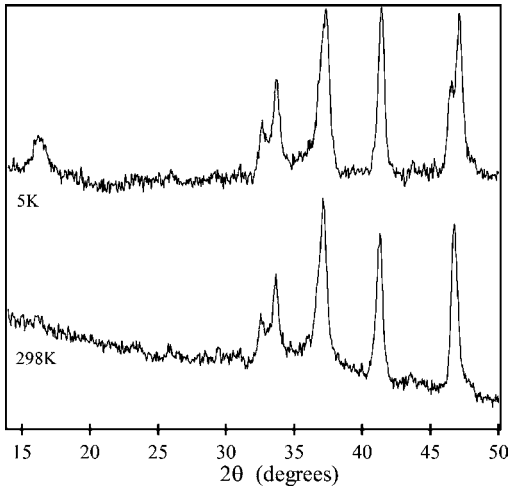

Figure 3. Neutron powder diffraction data (D2b) collected from $Sr_3Co_2O_4Cl_2$ at 298 and 5 K. An additional peak at $2\theta \sim 16°$ indicates long-range magnetic order at low temperature.

additional diffraction features could be readily indexed using an expanded $a_{mag} \approx \sqrt{2}a_{cryst}$, $b_{mag} \approx \sqrt{2}b_{cryst}$, $c_{mag} = c_{cryst}$ monoclinic unit cell, with the magnetic scattering intensity best accounted for by a model in which spins on neighboring cobalt centers within each CoO_2 sheet are aligned antiferromagnetically and spins on cobalt centers in adjacent sheets aligned ferromagnetically. The spins on the cobalt centers are aligned parallel or antiparallel to the z-axis with an ordered moment of 3.60 μ_B per cobalt center as shown in Figure 4. Full details of the refined magnetic model are given in the Supporting Information.

Variable Temperature Behavior. Neutron powder diffraction data (POLARIS) were collected as a function of temperature to monitor the evolution of the orthorhombic structural distortion and magnetic order present in $Sr_3Co_2O_4Cl_2$. Examination of these data revealed that, as shown in Figure 5c, the ordered magnetic moment on each cobalt center declines with increasing temperature, consistent with a magnetic ordering temperature of $T_N \sim 50$ K.

Magnetization data collected from $Sr_3Co_2O_4Cl_2$ using the "ferromagnetic subtraction" technique are shown in Figure 5a,b. The paramagnetic susceptibility of $Sr_3Co_2O_4Cl_2$ can be fitted to the Curie–Weiss law $[\chi = C/(T - \theta)]$ in the temperature range 50 < T/K < 300 to yield values of C = 4.53(3) cm^3 K mol^{-1} and

dx.doi.org/10.1021/ja306683y | J. Am. Chem. Soc. 2012, 134, 15946–15952

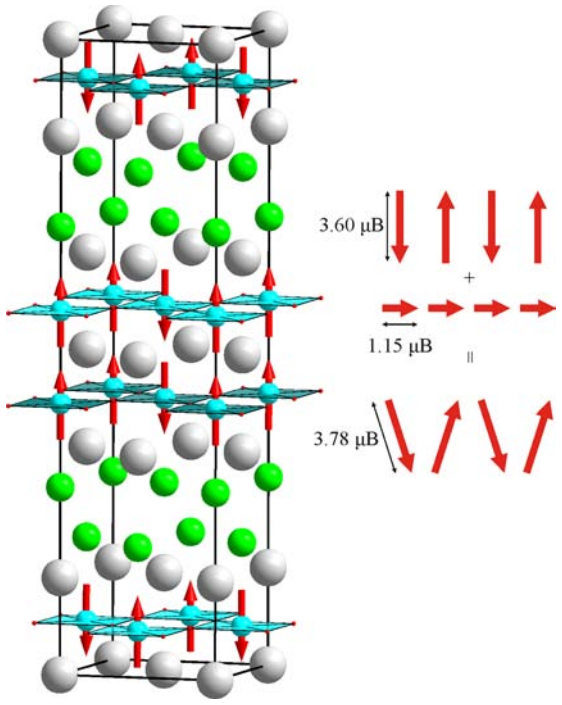

Figure 4. The antiferromagnetically ordered structure of $Sr_3Co_2O_4Cl_2$. Magnetization measurements indicate a saturated ferromagnetic moment of 1.15 μ_B per cobalt center at 5 K consistent with significant canting of the cobalt spins (Figure 5b). Combining the antiferromagnetic and ferromagnetic components of the canted system yields a total moment of 3.78 μ_B, a value significantly larger than expected from a spin-only Co(II) system.

θ = +2.94(3) K, where mol^{-1} means per mole of formula units of $Sr_3Co_2O_4Cl_2$. The observed value of the Curie constant is significantly higher than would be expected for a spin-only Co(II) system, even when the ~10% Co^{3+} $Sr_3Co_2O_5Cl_2$ secondary phase is taken into account ($C_{expected}$ = 3.98 cm^3 K mol^{-1}). At lower temperatures the paramagnetic susceptibility goes through a maximum at $T \sim 35$ K and there is a large increase in the saturated ferromagnetic moment at $T \sim 50$ K (Figure 5b), indicating the onset of magnetic order and consistent with the appearance of magnetic scattering in the low-temperature neutron diffraction data in this temperature range. The large increase in the saturated ferromagnetic moment of the sample associated with the appearance of magnetic order (1.15 μ_B per cobalt more at 5 K compared to 100 K) indicates a significant canting of the antiferromagnetically ordered cobalt spins. However, attempts to incorporate this canting into the refined magnetic model were unsuccessful due to the low number of magnetic diffraction reflections. Combining the ordered moment at 5 K (3.60 μ_B) and the saturated ferromagnetic moment at 5 K (1.15 μ_B) as a vector sum yields a total moment of 3.78 μ_B (Figure 4). This value is again much larger than the 3 μ_B expected for a spin-only d^7, $S = {}^3/_2$ Co(II) system, indicating a significant orbital contribution to the magnetism.

Figure 5d shows a plot of $(b/a) - 1$ obtained from structural refinement against neutron (POLARIS) and laboratory X-ray powder diffraction data sets, which clearly shows the orthorhombic distortion persists to $T \sim 200$ K, a temperature significantly higher than the magnetic ordering temperature.

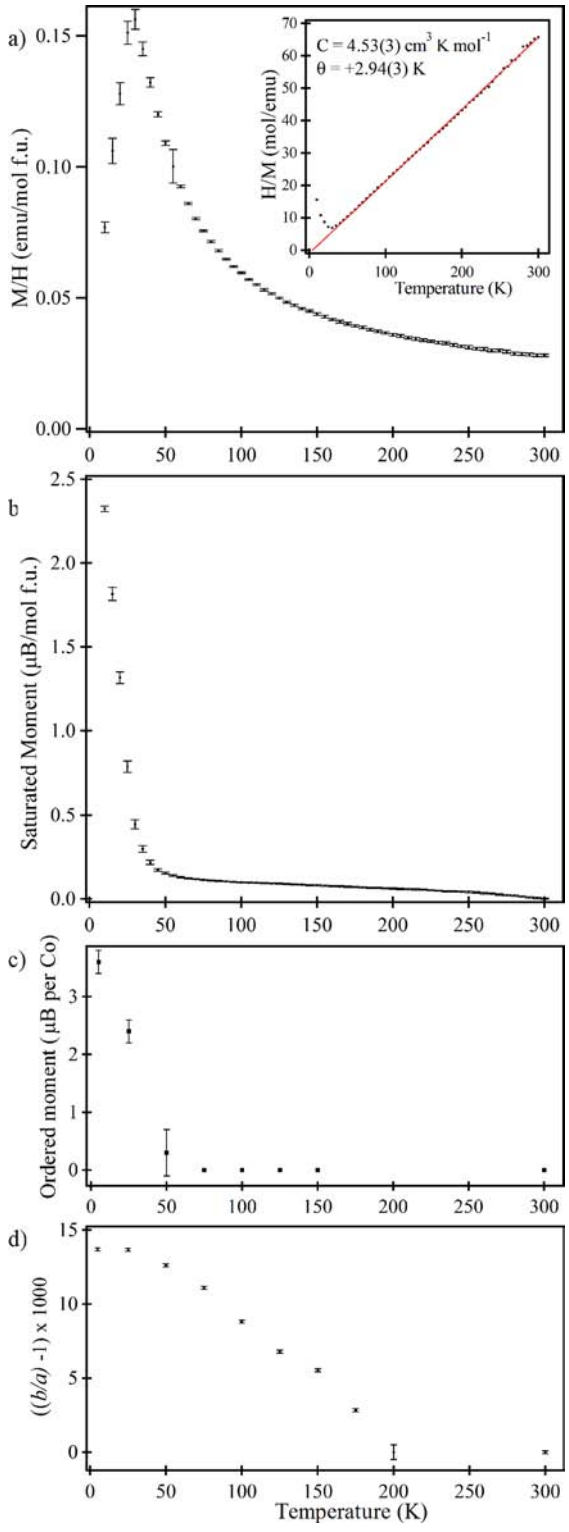

Figure 5. (a) The paramagnetic susceptibility, (b) the saturated ferromagnetic moment, and (c) the ordered antiferromagnetic moment determined by neutron diffraction of $Sr_3Co_2O_4Cl_2$ plotted as a function of temperature. (d) A plot of $(b/a) - 1$ against temperature as a measure of the orthorhombic distortion of $Sr_3Co_2O_4Cl_2$.

DISCUSSION

Reaction of $Sr_3Co_2O_5Cl_2$ with NaH leads to the formation of the Co(II) phase $Sr_3Co_2O_4Cl_2$. The reduction reaction

dx.doi.org/10.1021/ja306683y | J. Am. Chem. Soc. 2012, 134, 15946−15952

proceeds via the topochemical deintercalation of oxide ions from the central bridging anion site of the oxide-chloride phase, in a manner directly analogous to that observed previously for $Sr_3Fe_{2-x}Co_xO_5Cl_2$ ($0 \leq x \leq 1$) phases,[4,5] to yield a material consisting of double sheets of apex-linked $Co^{II}O_4$ square planes stacked with SrCl rocksalt layers (Figure 1).

The invariance of the structural selectivity of the topochemical reduction reactions of $Sr_3B_2O_5Cl_2$ phases to the identity of the transition metal B-cations reinforces the idea presented previously that it is the lattice structure of the $Sr_3B_2O_5Cl_2$ phases that directs the structural progression of these reduction reactions, rather than the electron configuration of the transition metal B-cation.[5] This feature of the reactions enables the electron count of the sheets of apex-linked BO_4 square planes to be tuned between d^6 (B = Fe) and d^7 (B = Co), allowing the evolution of the physical behavior of materials with this unusual metal−oxygen framework to be studied as a function of electron count.

Structural Lattice Distortion. The CoO_2 sheets of apex-linked $Co^{II}O_4$ square planes present in the 298 K structure of "double-layer" $Sr_3Co_2O_4Cl_2$ are very similar to those observed in the "single-layer" phases $Sr_2CoO_2Cl_2$ and $Ba_2CoO_2Cu_2S_2$,[13,14] with similar in-plane bond lengths for all three phases [Co−O: $Sr_3Co_2O_4Cl_2$ = 2.006(1) Å; $Sr_2CoO_2Cl_2$ = 2.030 Å; $Ba_2CoO_2Cu_2S_2$ = 2.032 Å].

On cooling below 200 K, $Sr_3Co_2O_4Cl_2$ is observed to undergo a tetragonal to orthorhombic structural distortion [structural distortion ratio, $(b/a - 1)$, $\sim 13.5 \times 10^{-3}$ at 5 K] with antiferromagnetic order observed below $T_N \sim 50$ K. In contrast, $Sr_2CoO_2Cl_2$ becomes magnetically ordered below $T_N \sim 215$ K and retains tetragonal symmetry down to the lowest temperature measured (20 K),[13] while $Ba_2CoO_2Cu_2S_2$ exhibits antiferromagnetic order below $T_N \sim 210$ K, before undergoing a small tetragonal to orthorhombic structural distortion below 155 K (distortion ratio $\sim 3.5 \times 10^{-3}$ at 5 K).[14]

Clarke et al. proposed that the tetragonal to orthorhombic lattice distortion observed on cooling $Ba_2CoO_2Cu_2S_2$ is due to magnetostriction and observed a strong correlation between the size of the ordered magnetic moment and the size of the lattice distortion in $(Sr_{1-x}Ba_x)_2CoO_2Cu_2S_2$ phases.[14] However, magnetostriction cannot account for the lattice distortion observed on cooling $Sr_3Co_2O_4Cl_2$ for a number of reasons: (i) The lattice distortion is observed to occur at a higher temperature than the onset of magnetic order ($T_{dist} \sim 200$ K, $T_N \sim 50$ K). (ii) The ordered magnetic moments in $(Sr_{1-x}Ba_x)_2CoO_2Cu_2S_2$ phases lie predominantly within the *xy*-planes of these phases, naturally breaking the tetragonal symmetry of the oxy−sulfide lattice; however, the ordered magnetic moments of $Sr_3Co_2O_4Cl_2$ principally point along the *z*-axis (Figure 4) making any symmetry breaking interaction weak. (iii) The size of the lattice distortion observed for $Sr_3Co_2O_4Cl_2$ at 5 K is approximately 5 times the size of that observed for $Ba_2CoO_2Cu_2S_2$, yet the size of the ordered magnetic moments of the two phases is approximately equal.

An alternative explanation for the observed lattice distortion can be found by examining the electronic structure of $Sr_3CoO_4Cl_2$. By analogy to the electronic structure calculated for the square planar Fe^{2+} centers in $SrFeO_2$,[15] the local electronic structure of the Co^{II} centers in $Sr_3Co_2O_4Cl_2$ is shown in Figure 6. The d^7, $S = {}^3/_2$ electronic configuration exhibits orbital degeneracy, with three electrons occupying the d_{xz}, d_{yz} degenerate orbital pair. The local electronic state of the Co^{II} centers is therefore unstable with respect to a structural

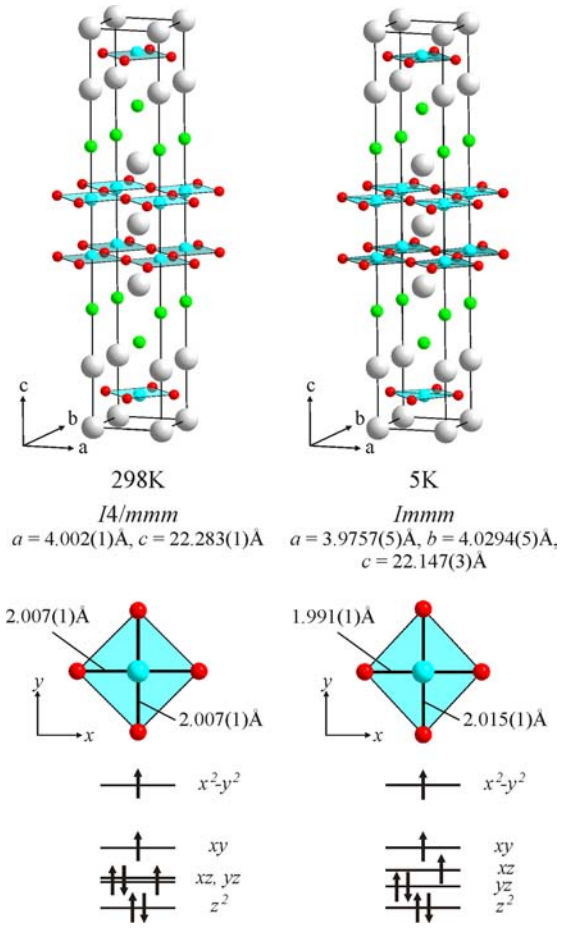

Figure 6. The structure of $Sr_3Co_2O_4Cl_2$ at 298 and 5 K (top). The local coordination geometry and local electronic state of cobalt centers at 298 and 5 K (bottom).

distortion which lifts the degeneracy of this state and thus lowers the energy of the system. As shown in Figure 6, the tetragonal to orthorhombic distortion observed on cooling $Sr_3Co_2O_4Cl_2$ below 200 K does indeed lift the degeneracy of the d_{xz}, and d_{yz} orbitals, consistent with this picture. We therefore propose that the symmetry-breaking transition observed on cooling $Sr_3Co_2O_4Cl_2$ is due to a Jahn−Teller-like distortion, which lifts the degeneracy of the local cobalt electronic configuration and thus lowers the energy of the whole system.

It should be noted that both $Sr_2CoO_2Cl_2$ and the $(Ba/Sr)_2CoO_2Cu_2S_2$ series of phases should also be unstable with respect to an analogous Jahn−Teller-type distortion, as they also have degenerate electronic states. That no such distortion is observed in these materials suggests that the elastic strain energy of the "single-layer" phases is too large to allow the lattice deformation to occur. Alternatively, interactions between the d_{xz} and d_{yz} orbitals of cobalt centers in adjacent CoO_2 layers of $Sr_3Co_2O_4Cl_2$ could lead to an amplification of the electronic stabilization achieved on distorting to an orthorhombic structure, providing another explanation for the differing behavior of the single and double layer phases.

Jahn−Teller distortions are commonly observed in oxide systems when octahedrally coordinated transition metal centers exhibit degenerate occupation of the e_g symmetry d-orbital set ($d_{x^2-y^2}$, d_{z^2}). Thus, for example, d^4, e_g^1 Cr^{2+} and Mn^{3+} centers or d^9, e_g^3 Cu^{2+} centers usually exhibit Jahn−Teller distortions in

dx.doi.org/10.1021/ja306683y | J. Am. Chem. Soc. 2012, 134, 15946−15952

complex oxide phases. This can be attributed to the strong interaction between the metal $d_{x^2-y^2}$ and d_{z^2} orbitals and O2p ligand orbitals with σ-type symmetry. In contrast, Jahn−Teller distortions are rarely seen when systems exhibit degenerate occupation of t_{2g} symmetry d-orbital set (d_{xz}, d_{yz}, d_{xy}) because the much weaker interaction between this set of orbitals and the π-symmetry O2p orbitals of the coordinating oxide ions means that any electronic stabilization gained on distortion due to the perturbation in d-orbital energies is rarely sufficient to overcome the bond/lattice energy lost by deforming the high symmetry crystal structure. As a result, Jahn−Teller distortions driven by the degeneracy of t_{2g} symmetry orbitals are usually only observed when the electronic stabilizing effect of the distortion is amplified by coupling to another electronic degree of freedom of the system. For example, $NaTiO_2$ and $NaVO_2$ exhibit Jahn−Teller distortions derived from t_{2g} orbital degeneracy (Ti^{3+} = d^1, t_{2g}^1; V^{2+} = d^2, t_{2g}^2) because the distortion not only lifts the degeneracy of the local transition metal electronic state but also distorts the triangular symmetry of the crystal structure, relieving the strong magnetic frustration observed in these two phases.[16,17] It is therefore rather surprising that $Sr_3Co_2O_4Cl_2$ exhibits a strong Jahn−Teller distortion driven by the degenerate occupation of π-symmetry d-orbitals (d_{xz}, d_{yz}) in the apparent absence of any other electronic coupling—a situation that clearly warrants further study.

Magnetic Behavior. Magnetization data collected from $Sr_3Co_2O_4Cl_2$ in the temperature range $50 < T/K < 300$ can be fitted to the Curie−Weiss law, consistent with paramagnetic behavior, and exhibit an effective moment of $\mu_{eff} = 4.25\ \mu_B$ per cobalt center (Figure 5a). Low-temperature neutron powder diffraction data indicate that $Sr_3Co_2O_4Cl_2$ adopts a canted antiferromagnetic ordered state below $T_N \sim 50$ K, in which the cobalt spins within each CoO_2 sheet align antiferromagnetically, with spins in adjacent sheets aligned ferromagnetically, as shown in Figure 4. This spin arrangement differs from that observed for the analogous iron phase, $Sr_3Fe_2O_4Cl_2$,[4] in which the interactions both within the FeO_2 sheets and between adjacent FeO_2 layers are antiferromagnetic. The change in the sign of the interlayer magnetic coupling interaction on substitution of iron with cobalt helps to explain the glassy magnetic behavior observed in $Sr_3Fe_{2-x}Co_xO_4Cl_2$ phases where $x \sim 1$,[5] by suggesting there is strong antiferromagnetic order within each $(Fe/Co)O_2$ sheet but that the interlayer interaction is a frustrated competition between antiferromagnetic and ferromagnetic order in the mixed cation systems.

The size of the high-temperature paramagnetic moment and the low-temperature ordered moment of $Sr_3Co_2O_4Cl_2$ are both significantly larger than would be expected from a simple $S = {}^3/_2$ spin-only system, suggesting a significant orbital contribution to the magnetic behavior. Clarke et al. have studied the orbital contribution to the magnetic moments of $Co^{II}O_4X_2$ (X = O, S, halogen) centers as a function of their coordination geometry and prepared a plot of the ordered moment against the ratio of (axial Co−X)/(equatorial Co−O) bond lengths.[14] Using this plot, a Co−Cl/Co−O ratio of 1.46 (Table 2) predicts an ordered moment of ~3.4 μ_B for $Sr_3Co_2O_4Cl_2$, compared to an observed ordered moment of 3.78 μ_B. This relatively large disagreement between predicted and observed values is most likely because the cobalt centers in $Sr_3Co_2O_4Cl_2$ are not really CoO_4X_2 centers but are instead CoO_4XCo centers [Co−Co = 3.20(1) Å] and the interaction between cobalt ions perturbs the d-orbital energies of the cobalt centers, resulting in a modified orbital contribution to the magnetic moment.

CONCLUSION

In conclusion, we have shown that by utilizing the structure-directing features of the $Sr_3B_2O_5Cl_2$ oxide−chloride framework to control the selectivity of reductive, topochemical, anion deintercalation reactions, a series of $Sr_3Fe_{2-x}Co_xO_4Cl_2$ ($0 < x < 2$) phases containing extended sheets of apex-linked $(Fe/Co)O_4$ square planes can be prepared, including the $x = 2$ end member $Sr_3Co_2O_4Cl_2$. The complete substitution of iron by cobalt adds one electron per transition metal center, resulting in a material, $Sr_3Co_2O_4Cl_2$, that has an orbitally degenerate local electronic state, which gives rise to an electronically driven lattice distortion at low temperature. Thus, by the controlled reduction of a carefully selected starting material we have prepared a novel phase with a highly unusual electronic structure that exhibits strong coupling between the structural lattice and the electronic configuration. By following a similar synthesis strategy a large number of other novel materials exhibiting complex correlated behavior should also be preparable.

ASSOCIATED CONTENT

Supporting Information

Description of the magnetic measurement procedure for samples containing elemental cobalt impurities; observed, calculated, and difference plots from the structural refinements of $Sr_3Co_2O_4Cl_2$ at 298 and 5 K; and a description of the magnetic refinement of $Sr_3Co_2O_4Cl_2$ against data collected at 5 K. This material is available free of charge via the Internet at http://pubs.acs.org.

AUTHOR INFORMATION

Corresponding Author

michael.hayward@chem.ox.ac.uk

Notes

The authors declare no competing financial interest.

ACKNOWLEDGMENTS

We thank R. Smith and E. Suard for assistance in collecting the neutron diffraction data. Experiments at the ISIS pulsed neutron facility were supported by a beam time allocation from the Science and Technology Facilities Council.

REFERENCES

(1) Hayward, M. A.; Green, M. A.; Rosseinsky, M. J.; Sloan, J. *J. Am. Chem. Soc.* **1999**, *121*, 8843.

(2) Seddon, J.; Suard, E.; Hayward, M. A. *J. Am. Chem. Soc.* **2010**, *132*, 2802.

(3) Dixon, E.; Hadermann, J.; Ramos, S.; Goodwin, A. L.; Hayward, M. A. *J. Am. Chem. Soc.* **2011**, *133*, 18397.

(4) Dixon, E.; Hayward, M. A. *Inorg. Chem.* **2010**, *49*, 9649.

(5) Dixon, E.; Hayward, M. A. *Inorg. Chem.* **2011**, *50*, 7250.

(6) Tsujimoto, Y.; Tassel, C.; Hayashi, N.; Watanabe, T.; Kageyama, H.; Yoshimura, K.; Takano, M.; Ceretti, M.; Ritter, C.; Paulus, W. *Nature* **2007**, *450*, 1062.

(7) Seinberg, L.; Yamamoto, T.; Tassel, C.; Kobayashi, Y.; Hayashi, N.; Kitada, A.; Sumida, Y.; Watanabe, T.; Nishi, M.; Ohoyama, K.; Yoshimura, K.; Takano, M.; Paulus, W.; Kageyama, H. *Inorg. Chem.* **2011**, *50*, 3988.

(8) Knee, C. S.; Field, M. A. L.; Weller, M. T. *Solid State Sci.* **2004**, *6*, 443.

(9) Grenier, J. C.; Ghodbane, S.; Demazeau, G.; Pouchard, M.; Hagenmuller, P. *Mater. Res. Bull.* **1979**, *14*, 831.
(10) Loureiro, S. M.; Felser, C.; Huang, Q.; Cava, R. *J. Chem. Mater.* **2000**, *12*, 3181.
(11) Larson, A. C.; Von Dreele, R. B. *Los Alamos Natl. Lab. [Rep.]* **2000**, 86−748.
(12) Hayward, M. A.; Rosseinsky, M. *J. Chem. Mater.* **2000**, *12*, 2182.
(13) Knee, C. S.; Weller, M. T. *Phys. Rev. B* **2004**, *70*, 144406.
(14) Smura, C. F.; Parker, D. R.; Zbiri, M.; Johnson, M. R.; Gal, Z. A.; Clarke, S. J. *J. Am. Chem. Soc.* **2011**, *133*, 2691.
(15) Xiang, H. J.; Wei, S.-H.; Whangbo, M. H. *Phys. Rev. Lett.* **2008**, *100*, 167207.
(16) Clarke, S. J.; Fowkes, A. J.; Harrison, A.; Ibberson, R. M.; Rosseinsky, M. *J. Chem. Mater.* **1998**, *10*, 372.
(17) McQueen, T. M.; Stephens, P. W.; Huang, Q.; Klimczuk, T.; Ronning, F.; Cava, R. *J. Phys. Rev. Lett.* **2008**, 101.